

Frequency metrology of helium around 1083 nm and determination of the nuclear charge radius

P. Cancio Pastor,^{1,2,*} L. Consolino,^{1,2} G. Giusfredi,^{1,2} P. De Natale,^{1,2} M. Inguscio,² V. A. Yerokhin,³ and K. Pachucki⁴

¹*Istituto Nazionale di Ottica-CNR (INO-CNR), Via Nello Carrara 1, I-50019 Sesto Fiorentino, Italy*

²*European Laboratory for Non-Linear Spectroscopy (LENS) and Dipartimento di Fisica, Università di Firenze
Via Nello Carrara 1, I-50019 Sesto Fiorentino, Italy*

³*St. Petersburg State Polytechnical University, Polytekhnicheskaya 29, St. Petersburg 195251, Russia*

⁴*Faculty of Physics, University of Warsaw, Hoza 69, 00-681 Warsaw, Poland*

We measure the absolute frequency of seven out of the nine allowed transitions between the 2^3S and 2^3P hyperfine manifolds in a metastable ^3He beam by using an optical frequency comb synthesizer-assisted spectrometer. The relative uncertainty of our measurements ranges from 1×10^{-11} to 5×10^{-12} , which is, to our knowledge, the most precise result for any optical ^3He transition to date. The resulting 2^3P - 2^3S centroid frequency is 276 702 827 204.8 (2.4) kHz. Comparing this value with the known result for the ^4He centroid and performing *ab initio* QED calculations of the ^4He - ^3He isotope shift, we extract the difference of the squared nuclear charge radii δr^2 of ^3He and ^4He . Our result for $\delta r^2 = 1.074(3) \text{ fm}^2$ disagrees by about 4σ with the recent determination [R. van Rooij *et al.*, *Science* **333**, 196 (2011)].

Spectacular progress of experimental techniques, achieved in the last decades, has made precision spectroscopy of light atoms a unique tool for the determination of fundamental constants and properties of atomic nuclei. The underlying theory, quantum electrodynamics (QED), allows one to calculate atomic properties *ab initio* and keep control of the magnitude of uncalculated effects. Possible discrepancies between theory and experiment may signal a lack of our knowledge of details of the interactions between electrons, nuclei, and other particles. An important recent example is the discrepancy of the proton charge radius derived from the spectroscopy of the electronic and muonic hydrogen [1]. This discrepancy is still unresolved and might lead to important consequences, such as a change of the accepted value for the Rydberg constant (which was, up to now, considered to be one of the best known fundamental constants) or discovery of unknown effects in the electromagnetic lepton-nucleus interaction.

Another important disagreement reported recently concerns the charge radii of helium isotopes. Specifically, the difference of the squares of the charge radii of the ^3He and ^4He nuclei determined from the 2^1S - 2^3S transition [2] was reported to differ by about 4 standard deviations (σ) from that derived using the 2^3P_0 - 2^3S transition [3]. In this Letter, we aim to resolve this discrepancy by performing an independent, high-precision measurement of the ^4He - ^3He isotope shift, on the one hand, and by advancing the theory of the helium isotope shift, on the other hand.

In the experimental part, we measure the absolute frequency of seven out of the nine allowed transitions between the 2^3S and 2^3P hyperfine manifolds of ^3He with a precision ranging from 1×10^{-11} to 5×10^{-12} . To the best of our knowledge, these are currently the most accurate measurements for any optical ^3He transition. In

the theoretical part, we perform a rigorous QED calculation of the isotope shift of the centroid of the 2^3P - 2^3S transition, identifying several corrections omitted in the previous studies and carefully examining the uncertainty due to uncalculated effects. Combining the experimental and theoretical results, we obtain the difference of the squares of the charge radii of the ^3He and ^4He nuclei. The improved theory is also applied for reexamination of the previous experimental result [2].

The structure of the 2^3S and 2^3P levels in ^3He and ^4He is shown in Fig. 1. In the following, we will use the shorthand notation $P_{J_P, F_P}^{F_S}$ to denote the $2^3S_{1, F_S} \rightarrow 2^3P_{J_P, F_P}$ hyperfine transition in ^3He and P_{J_P} to denote the $2^3S_1 \rightarrow 2^3P_{J_P}$ transition in ^4He . We now address the measurement procedure applied to the seven transitions between the 2^3S and 2^3P hyperfine manifolds of ^3He . The remaining two allowed transitions, $P_{1,3/2}^{1/2}$ and $P_{2,3/2}^{3/2}$, have a very weak intensity due to the hyperfine suppression [4, 5], which prohibits their measurement with our spectroscopic setup.

Multiresonant precision spectroscopy was performed by using the optical frequency comb synthesizer (OFCS)-assisted laser system at 1083 nm described in Ref. [6]. In each run, quasisimultaneous saturation spectra of two out of these seven hyperfine transitions were recorded in an absolute frequency scale, and the frequency center was measured by a fitting procedure [6]. In this way, absolute frequencies of each transition and their differences are measured minimizing possible time-dependent systematic errors. This procedure is repeated for about 200 runs for each transition. During these runs, different transitions were coupled to each other, and for each couple the multiresonant probe laser system was interchanged, in order to randomize, as much as possible, the measurement procedure. The final results, together with

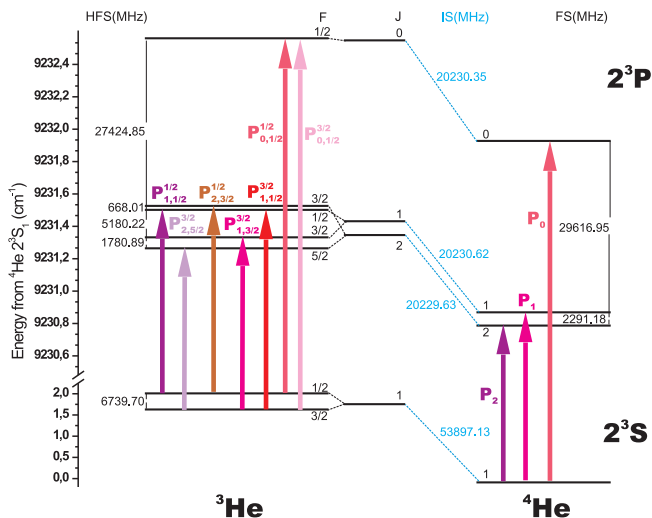


FIG. 1. (color online) Level scheme of the 2^3S and 2^3P manifolds of ^3He and ^4He isotopes. ^3He HFS, ^4He fine structure (FS) and ^4He - ^3He IS splittings are shown.

TABLE I. Absolute frequency measurements of $P_{J,F}^{F_S}$ ^3He hyperfine transitions: statistical results and systematic error budget, in kHz. Uncertainties are given in parentheses.

Transition	Statistical value ^a	Zeeman ^b shift	Final ^c result
$P_{1,1/2}^{1/2}$	276 698 164 610.4(1.8)	(0.233)	276 698 164 610.4(2.0)
$P_{2,5/2}^{3/2}$	276 698 611 209.1(3.1)	(0.148)	276 698 611 209.1(3.2)
$P_{2,3/2}^{1/2}$	276 698 832 617.9(2.5)	(0.303)	276 698 832 617.9(2.5)
$P_{1,3/2}^{3/2}$	276 700 392 099.8(0.9)	(0.369)	27 6 700 392 099.8(1.3)
$P_{1,1/2}^{3/2}$	276 704 904 311.7(2.3)	(0.233)	276 704 904 311.7(2.4)
$P_{0,1/2}^{1/2}$	276 726 257 468.9(1.1)	(0.932)	276 726 257 468.9(1.7)
$P_{0,1/2}^{3/2}$	276 732 997 170.4(2.3)	(0.466)	276 732 997 170.4(2.5)

^a Each measurement was corrected by the day-by-day RS+LS+2DS shifts (see text for details).

^b Because of residual magnetic fields ($< 0.03 \mu\text{T}$).

^c The OFCS error of $10^{-12} \times$ statistical value (kHz) and the 1DS error of 0.8 kHz were added in quadrature in the final uncertainty.

the error budget, are summarized in Table I.

Particular attention was paid to single out and quantify possible systematic errors. As in our previous ^4He measurements [7, 8], the main systematic correction was due to recoil-induced mechanical shift (RS) [9]. As in that case, we calculate its contribution for each transition by solving the atomic Bloch equations, including ac Stark shift [light shift LS], and taking into account the atom dynamics during interaction with the laser, in the present experimental conditions. Second-order Doppler (2DS) correction due to the longitudinal velocity distribution of the atoms in the ^3He metastable beam was also included in this calculation. Since RS is like an accumulated recoil during laser-atom interaction time, it is strongly dependent on the metastable atomic flux in our

experimental setup, and hence on the dc discharge conditions used to metastabilize the ^3He atomic beam. We have noticed that such conditions changed during a day of measurements, due to progressive saturation of the filtering system for contaminant gases, used in the ^3He gas recycling line inserted in the atomic beam. In fact, we monitored this change by measuring the atomic longitudinal velocity distribution behavior during a day. From this data, an averaged longitudinal velocity distribution for each day is determined, which enters as a parameter in the RS+LS+2DS calculation. All measurements for each transition are corrected by the corresponding day shift. The final frequency is calculated as a statistical average of all corrected measurements performed for each transition. Such a procedure is shown in Fig. 2 for the $P_{2,3/2}^{1/2}$ transition, where about 180 measurements without (squares) and with (circles) RS+LS+2DS day-shift corrections are reported. As a result, a Gaussian distribution of the corrected measurements is shown in the fill-bar graph of Fig.2, witnessing that our data have “white” statistical fluctuations.

Systematics uncertainties due to first-order Doppler shift (1DS), OFCS accuracy, and Zeeman shift, have been added in quadrature to the statistical one, as shown in Table I. 1DS was avoided due to the saturation spectroscopy configuration [7], but with an error of 0.8 kHz, due to the achievable angular accuracy between the forward and the backward interacting laser beams. The Rb-GPS disciplined quartz oscillator, used in our OFCS, guarantees a relative accuracy of 10^{-12} , considered in the error budget. Finally, a residual magnetic field in the atom-laser interaction region lower than $0.03 \mu\text{T}$, gives a Zeeman shift uncertainty for each transition (Table I, third column), without shifting the transition barycenter. The total accuracy of our measurements, summarized in Table I, ranges from 1×10^{-11} to 5×10^{-12} , which is currently the best reported result for any optical transition in ^3He .

An independent check for the accuracy of our measurements is made by extracting the known value of the hyperfine splitting (HFS) of the metastable 2^3S state from the transitions in Table I. The two differences $P_{0,1/2}^{1/2} - P_{0,1/2}^{3/2}$ and $P_{1,1/2}^{1/2} - P_{1,1/2}^{3/2}$ yield the values of 6 739 701.5 (3.0) and 6 739 701.3(3.1) kHz, respectively, which are consistent with each other and in perfect agreement with the more accurate result of 6739701.177 (16) kHz [10].

Comparison of our measurements with the previous experimental results is given in Table II. The centroid values of the 2^3P and 2^3S energies are defined as an average over all fine and hyperfine sublevels,

$$E(2^3L) = \frac{\sum_{J,F} (2F+1) E(2^3L_{J,F})}{(2I+1)(2S+1)(2L+1)}, \quad (1)$$

where $2^3L = 2^3S$ and 2^3P for $L=0$ and 1 , respectively.

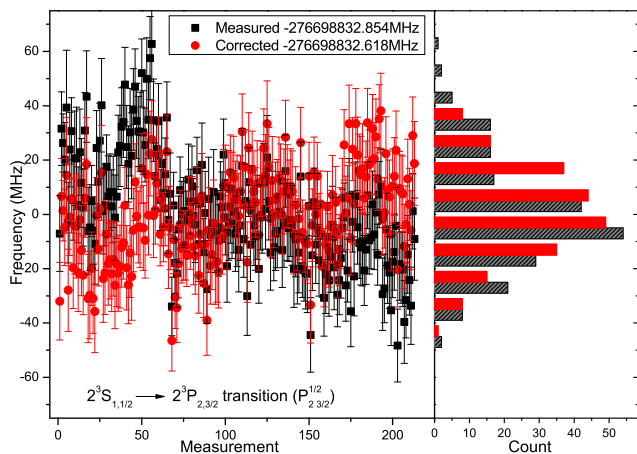


FIG. 2. (color online) Day-by-day correction of the RS+LS+2DS shift for the measurements of the $P_{2,3/2}^{1/2}$ hyperfine transition. Left graph: the squares (black) are the measured data, and the circles (red) are the corrected data. A different mean frequency was subtracted to bring data in the same frequency vertical scale for a clear comparison. Right graph: bar graph distribution of the measured (dashed black bars) and corrected (fill red bars) frequencies.

TABLE II. Comparison with prior measurements, in kHz.

$^3\text{He } 2^3P-2^3S$ centroid	276 702 827 204.8 (2.4)	
	276 702 827 145 (77) ^a	
$^4\text{He } 2^3P-2^3S$ centroid	276 736 495 649.5 (2.1)	[7]
	276 736 495 580 (70)	[11]
$^4\text{He } P_2-^3\text{He } P_{0,1/2}^{3/2}$	810 594.3 (3.3) ^b	
	810 599 (3)	[3]
	810 608 (30)	[12]
$^3\text{He } P_{0,1/2}^{3/2}-^4\text{He } P_1$	1 480 582.1 (3.2)	
	1 480 573 (30)	[12]

^a Evaluated by combining the $^4\text{He } P_2$ frequency [11], the $^4\text{He}-^3\text{He } P_2-P_{0,1/2}^{3/2}$ interval [3], the $^3\text{He } 2^3S$ HFS [10], and the 2^3P HFS [15].

^b Evaluated by combining the $P_{0,1/2}^{3/2}$ interval from Table I, the P_0 frequency [7], and the $2^3P_0-2^3P_2$ interval [13].

To the best of our knowledge, there are no published measurements of 2^3P-2^3S HFS frequencies. Therefore, we obtain the “previous experimental value” of the $^3\text{He } 2^3P-2^3S$ centroid frequency as a combination of several experiments and the calculated HFS intervals (see footnote in Table II). The previous result is in agreement with our measurement but 33 times less accurate. The $^4\text{He } 2^3P-2^3S$ centroid was measured by us previously [7], in agreement with the independent determination by Shiner *et al.* [11]. In order to check the consistency of our present measurements on ^3He with our previous measurements for ^4He [7], in Table II, a comparison of the frequency differences of the $^3\text{He } P_{0,1/2}^{3/2}$ and the $^4\text{He } P_1$

TABLE III. $^4\text{He}-^3\text{He}$ isotope shift of the centroid energies, for the pointlike nucleus, in kHz. m_r is the reduced mass and M is the nuclear mass.

Contribution	2^3P-2^3S	2^1S-2^3S
$m_r \alpha^2$	12 412 458.1	8 632 567.86
$m_r \alpha^2 (m_r/M)$	21 243 041.3	-608 175.58
$m_r \alpha^2 (m_r/M)^2$	13 874.6	7 319.80
$m_r \alpha^2 (m_r/M)^3$	4.6	-0.30
$m_r \alpha^4$	17 872.8	8 954.22
$m_r \alpha^4 (m_r/M)$	-20 082.4	-6 458.23
$m_r \alpha^4 (m_r/M)^2$	-3.0	-1.84
$m \alpha^5 (m/M)$	-60.7	-56.61
$m \alpha^6 (m/M)$	-15.5 (3.9)	-2.75 (69)
Nuclear polarizability	-1.1 (1)	-0.20 (2)
HFS mixing	54.6	-80.69
Total	33 667 143.2 (3.9)	8 034 065.69 (69)
Other theory [15, 16] ^a	33 667 146.2 (7)	8 034 067.8 (1.1)

^a Corrected by adding the triplet-singlet HFS mixing.

and P_2 intervals with independent measurements [3, 12] is reported.

The difference of our results for the 2^3P-2^3S centroid energy in ^3He and ^4He yields the experimental value of the isotope shift (IS). Combined with theoretical calculations, the experimental IS can be used [14] to determine the difference of the squared nuclear charge radii, $\delta r^2 \equiv r^2(^3\text{He}) - r^2(^4\text{He})$.

Numerical results of our calculation of the IS of the 2^3P-2^3S and 2^1S-2^3S transitions for the point nucleus are presented in Table III. As compared to the previous evaluations [15, 16], the higher-order recoil [$m_r \alpha^2 (m_r/M)^3$ and $m_r \alpha^4 (m_r/M)^2$] and the nuclear polarizability corrections were accounted for and the higher-order QED effects [$m \alpha^6 (m/M)$] were estimated more carefully. The calculation extends our previous works [17, 18]; its details will be reported elsewhere. The total uncertainty comes from the uncalculated higher-order QED effects. Note that it is much larger than the one reported previously in Ref. [15].

Our definition of the IS differs from that used previously [2, 3] by the fact that we average out not only the hyperfine but also the fine-structure splitting. The advantage of using the centroid energy is that theory becomes much more transparent and can be directly compared to the experiment.

The difference of the theoretical point-nucleus results in Table III and the experimental IS comes from the finite nuclear size (FNS) effect, which can be parametrized as

$$\delta E_{\text{FNS}} = \frac{2\pi}{3} Z\alpha m_r^3 r^2 \langle \delta^{(3)}(r_1) + \delta^{(3)}(r_2) \rangle \times \left[1 - (Z\alpha)^2 \ln(Z\alpha r) + (Z\alpha)^2 f_{\text{rel}} \right], \quad (2)$$

where f_{rel} is the relativistic correction beyond the leading logarithm. The FNS contribution can be represented

as $\delta E_{\text{FNS}} = Cr^2$, where the coefficient C , according to the above equation, depends very weakly on r . Our calculated values for the coefficient C are

$$C(2^3P - 2^3S) = -1212.2(1) \text{ kHz/fm}^2, \quad (3)$$

$$C(2^1S - 2^3S) = -214.69(1) \text{ kHz/fm}^2, \quad (4)$$

which can be compared with the previous results $C(2^3P - 2^3S) = -1209.8$ [19] and $C(2^1S - 2^3S) = -214.40$ [20].

At present, there are three independent measurements of the ^4He - ^3He IS that can be used to infer δr^2 with a comparable accuracy, our experiment and those of Refs. [2, 3]. Our theory, summarized in Table III, allows us to extract the charge radius difference δr^2 consistently from the present experiment and that of Ref. [2]. The results are

$$\delta r^2(\text{this work}) = 1.074(3) \text{ fm}^2, \quad (5)$$

$$\delta r^2([2], \text{reevaluated}) = 1.028(11) \text{ fm}^2. \quad (6)$$

The δr^2 value of Eq. (6) is by about 1σ larger than that given in Ref. [2], $1.019(11) \text{ fm}^2$, because of the change in the theoretical IS value. Using Eq. (5) and the nuclear charge radius of ^4He [21], we obtain the root-mean-square radius of the ^3He isotope to be $1.975(4) \text{ fm}$.

The results of Eqs. (5) and (6) can be also compared with the determination by Shiner *et al.*,

$$\delta r^2([3]) = 1.059(3) \text{ fm}^2. \quad (7)$$

which used the older isotope shift theory. We do not reevaluate this result here, since it would require improvement in theoretical predictions for HFS intervals.

We observe, as shown in Fig.3, that the above results for the radius difference δr^2 are inconsistent with each other. In particular, a 4σ discrepancy is present between our value and that of Ref. [2], for which we do not have a satisfactory explanation at present. Note that both experiments use the same OFCS assisted laser technology, that most of the theoretical contributions are checked by independent calculations, and that the determination of the charge radius difference is now performed consistently within the same theory. The observed discrepancy may be in principle explained by some hidden systematics in experiments or by yet unknown effects in the electron-nucleus interaction.

The possibility that some additional effects beyond the standard QED exist has been discussed in the literature ever since the muonic hydrogen experiment [1] raised what is now known as the proton charge radius puzzle. One of the ways for solving this puzzle is to investigate similar systems, aiming to confirm or to disprove the disagreement observed for hydrogen. In the present Letter, we report a 4σ discrepancy for the nuclear charge radius difference of ^3He and ^4He .

Precision spectroscopic determination of the nuclear charge radii of the helium isotopes becomes today of

particular importance, as the next goal of the muonic

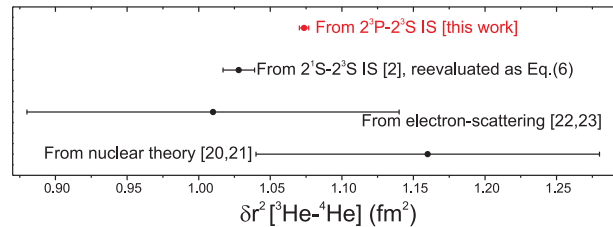


FIG. 3. (color online) Different determinations of the difference of the squared nuclear charge radii for ^3He and ^4He .

hydrogen group from the Paul Scherrer Institute is the measurement of the Lamb shift in muonic helium [24]. This experiment will provide an independent determination of the charge radii of helium isotopes and will allow one to compare the results obtained by the spectroscopy of the electronic and muonic atoms, thus hopefully shedding light on the proton charge radius problem and on the discrepancy for the helium charge radius difference.

* pablo.canciopastor@ino.it

- [1] R. Pohl *et al.*, Nature (London) **466**, 213 (2010).
- [2] R. van Rooij *et al.* Science **333**, 196 (2011).
- [3] D. Shiner, R. Dixon, and V. Vedantham, Phys. Rev. Lett. **74**, 3553 (1995).
- [4] I. A. Sulai *et al.* Phys. Rev. Lett. **101**, 173001 (2008).
- [5] L. Consolino *et al.*, to be published.
- [6] L. Consolino *et al.* Opt. Express **19**, 3155 (2011).
- [7] P. Cancio Pastor *et al.* Phys. Rev. Lett. **92**, 023001 (2004), [(E) *ibid* **97**, 139903 (2006)].
- [8] G. Giusfredi *et al.* Can. J. Phys. **83**, 301 (2005).
- [9] F. Minardi *et al.*, Phys. Rev. A **60**, 4164 (1999).
- [10] S. D. Rosner and F. M. Pipkin, Phys. Rev. A **1**, 571 (1970), [(E) *ibid* **3**, 521 (1971)].
- [11] D. Shiner, R. Dixon, and P. Zhao, Phys. Rev. Lett. **72**, 1802 (1994).
- [12] P. Zhao, J.R. Lawall, and F.M. Pipkin, Phys. Rev. Lett. **66**, 592 (1991).
- [13] M. Smiciklas and D. Shiner, Phys. Rev. Lett. **105**, 123001 (2010).
- [14] F. Marin *et al.* Phys. Rev. A **49**, R1523 (1994).
- [15] D.C. Morton, Q. Wu, and G. W. F. Drake, Can. J. Phys. **84**, 83 (2006).
- [16] G. W. F. Drake, priv. comm., 2010, as cited in [2].
- [17] K. Pachucki and V. A. Yerokhin, Phys. Rev. A **79**, 062516 (2009), [*ibid.* **81**, 039903(E) (2010)].
- [18] K. Pachucki and V. A. Yerokhin, Phys. Rev. Lett. **104**, 070403 (2010).
- [19] D.C. Morton, Q. Wu, and G. W. F. Drake, Phys. Rev. A **73**, 034502 (2006).
- [20] G. Drake, W. Nörtershäuser, and Z.-C. Yan, Can. J. Phys. **83**, 311 (2005).
- [21] I. Sick, Phys. Rev. C **77**, 041302 (2008).
- [22] A. Kievsky *et al.* J. Phys. G **35**, 063101 (2008).
- [23] I. Sick, Lect. Notes Phys. **745**, 57 (2008).
- [24] A. Antognini *et al.*, Can. J. Phys. **89**, 47 (2011).